Exposing the Sunda shelf: Tropical responses to eustatic sea level change

Andrew B. G. Bush
Department of Earth and Atmospheric Sciences, University of Alberta, Edmonton, Alberta, Canada

Richard G. Fairbanks
Department of Earth and Environmental Sciences of Columbia University and Lamont Doherty Earth Observatory, Palisades, New York, USA

Received 8 October 2002; revised 15 January 2003; accepted 26 March 2003; published 2 August 2003.

[1] During the last glacial period, eustatic lowering of sea level exposed large areas of continental shelves that are presently submerged. By a series of direct numerical simulations we investigate the sensitivity of the atmosphere-ocean system to exposure of the extensive Sunda shelf in the western tropical Pacific. We demonstrate that this specific forcing factor triggers increased convection and upper level divergence over the shelf itself, an increased Walker circulation over the far western Pacific, and subsidence over the central and eastern Pacific that weakens the surface easterlies. A comparison of atmosphere-only with coupled atmosphere-ocean integrations demonstrates that dynamic coupling of the ocean enhances the equatorial response, with cooling and drying of the tropics north and south of the Intertropical Convergence Zone. Exposure of the shelf therefore represents one mechanism by which glacial climates are affected by eustatic sea level changes. These changes constitute a fundamental shift in the El Niño background state. *INDEX TERMS:* 1620 Global Change: Climate dynamics (3309); 3319 Meteorology and Atmospheric Dynamics: General circulation; 3339 Meteorology and Atmospheric Dynamics: Ocean/atmosphere interactions (0312, 4504); 3344 Meteorology and Atmospheric Dynamics: Paleoclimatology; *KEYWORDS:* Sunda shelf, tropical climate variability, ENSO (El Niño and La Niña), eustatic sea level, Last Glacial Maximum, tropical Pacific

Citation: Bush, A. B. G., and R. G. Fairbanks, Exposing the Sunda shelf: Tropical responses to eustatic sea level change, *J. Geophys. Res.*, *108*(D15), 4446, doi:10.1029/2002JD003027, 2003.

1. Background and Introduction

[2] Changes in global mean sea level have played a fundamental role in determining our planet's climatic history and in regulating exposure of land connections between continents. Not only do these continental gateways control terrestrial migratory routes [*Hallam*, 1994], they also contribute to determining the planet's global mean albedo and hence the net radiation budget and surface equilibrium temperature. During glacial periods when sea level is low, for example, the Indonesian archipelago becomes a unified landmass through exposure of the massive Sunda shelf that today lies submerged in approximately 70 meters of the western Pacific Ocean [*Smith and Sandwell*, 1997; *Fairbanks*, 1989]. This shelf is one of the world's largest in areal extent (approximately 2.1×10^6 km^2) and stretches southward from the Indochina peninsula across the equator to Java.

[3] Stability of tropical temperatures through the last glacial cycle has been debated extensively [*Guilderson et al.*, 1994; *Stute et al.*, 1995; *Broecker*, 1986; *Lyle et al.*, 1992; *Hostetler and Mix*, 1999; *Lea et al.*, 2000]. Since the tropical atmosphere is particularly sensitive to anomalous heat sources or sinks [*Gill*, 1980; *Keshavamurty*, 1982; *Sardeshmukh and Hoskins*, 1988], exposure of the Sunda shelf has the potential to produce strongly nonlocal effects through the atmosphere's large-scale Rossby and Kelvin wave responses. Exposure of the shelf also reduces the areal extent of the West Pacific Warm Pool and therefore impacts the amount of available moisture [*Pelejero et al.*, 1999]. The rapidity with which eustatic sea level changes would cause flooding or exposure [*Fairbanks*, 1989, 1990] means that any climatological changes would occur on the same timescale as the flooding (as short a time as 300 years [*Hanebuth et al.*, 2000]) and that they may play an important role in governing climatological tropical temperatures and precipitation patterns [*Quinn*, 1971; *Colinvaux*, 1972].

[4] To address this issue, we compared the results of four numerical simulations. Two simulations were performed with an atmospheric general circulation model (GCM) [*Gordon and Stern*, 1982] with specified sea surface temperature (SST). The first simulation was a control experiment that incorporated modern values of sea level and continental exposure. Configuration of the second simulation was identical except for the Sunda shelf itself, which was exposed as a tropical landmass (Figure 1). In reality, other large continental shelves (such as that in the Gulf of

0148-0227/03/2002JD003027$09.00

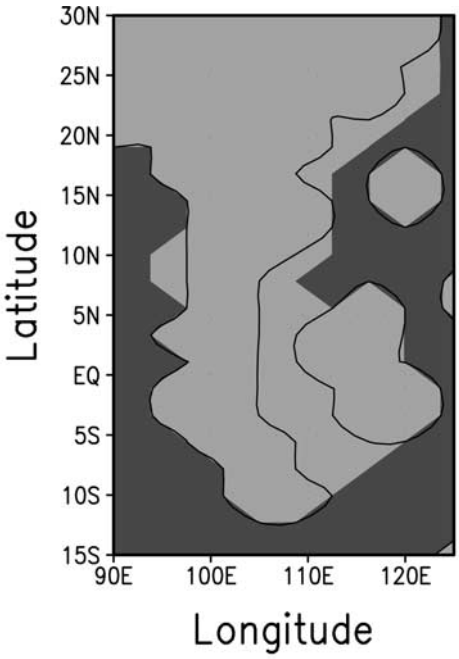

Figure 1. The continental margins used in the four experiments. The contour line indicates the modern margin of the control experiments. Light shading indicates the margin when the Sunda shelf is exposed.

Carpentaria) would also be exposed during a eustatic lowering of sea level. For the purposes of this study the effect of the Sunda shelf is examined in isolation. However, in comparing these results to those of the Last Glacial Maximum (LGM) simulation of *Bush and Philander* [1999] it should be kept in mind that all continental shelves above 120 m depth were exposed in the latter simulation.

[5] The equivalent spatial resolution of the model was 3.75° in longitude and approximately 2° in latitude. There were 14 levels in the vertical with the lowest level at approximately 30 meters above the ground and the highest level at 50 millibars. Global SSTs were prescribed daily from climatological data [*Levitus*, 1982] and were the same in both simulations (except over the Sunda shelf, where SST is not prescribed in the second simulation). The exposed shelf was assigned surface albedos equal to the zonal average of all land point albedos at that latitude. The shelf therefore has albedo values that are representative of tropical vegetation, and should therefore act as a trigger for tropical convection. Orbital parameters were set to modern values in both simulations.

[6] The second two simulations were performed with a coupled atmosphere-ocean GCM that uses the same atmospheric model but includes a dynamic ocean model [*Bush and Philander*, 1999]. Configuration differences between these two simulations were the same as in the atmosphere-only cases with the addition that ocean bathymetry in the Sunda shelf region was also modified to be consistent with Figure 1. Initial ocean conditions were taken from Levitus data [*Levitus*, 1982], and modern orbital forcing is applied. Time averages shown in subsequent figures were taken from 10 years of the atmosphere-only simulations and from the last 40 years of the 50-year coupled model integrations. Adjustment of the tropical atmosphere to the exposed landmass occurs very rapidly through the atmospheric Rossby and Kelvin wave responses (discussion to follow); consequent changes in the tropical Pacific thermocline and SST evolve through the first ten years of the simulation by the wind-driven dynamics that govern in this region [*Philander*, 1990]. Changes in the climatological mean state of the tropics are statistically significant, by a t test, at more than the 99% level. Note that the simulations are not capable of determining the impact of these changes on deep water formation or benthic currents. Models that focus on the thermohaline circulation can preclude realistic tropical thermocline processes by virtue of the unrealistically high vertical diffusivities required to produce the global overturning circulation [*Meehl et al.*, 2001]. In this model we employ a vertical mixing scheme, based on the Richardson number, that has been shown to improve tropical climatology and interannual dynamics by keeping the flow below the mixed layer as adiabatic as possible [*Pacanowski and Philander*, 1981].

[7] These sensitivity experiments are designed to determine, in isolation, the effect of shelf exposure. As such, they are similar in methodology to the experiments of *Broccoli and Manabe* [1987] in which other LGM forcing factors (ice sheets, carbon dioxide, and land surface albedo) were determined in isolation. A direct comparison of the following results to proxy data is not therefore warranted. However, comparison to the LGM simulation of *Bush and Philander* [1999], in which many forcing factors were at play (shelf exposure, carbon dioxide, orbital changes, ice sheets, etc.), allows the relative role of Sunda shelf exposure in the total tropical climate change to be determined.

2. Results

[8] Exposure of the Sunda shelf triggers similar atmospheric responses in both atmosphere-only and coupled simulations. In particular, there is enhanced low-level convergence induced by surface heating over the shelf itself (Figure 2). Anomalous easterly winds over the western Pacific (between 135°E and 150°W in the atmosphere-only simulation) are more limited in spatial extent in the coupled model (110°–130°E) because of the southerly cross-equatorial flow (from 140°E to 90°W) that arises from coupled atmosphere-ocean interactions to be described below.

2.1. Atmospheric Response

[9] Anomalous westerly winds occur over the far eastern Pacific when the shelf is exposed. These winds are caused by enhanced subsidence and surface divergence over the central Pacific, as is seen more clearly in the Walker circulation anomalies (Figure 3). The Pacific Walker cell in the (atmosphere-only) control simulation is located between the longitudes of 120°E and 80°W (Figure 3a; the stream function definition of the Walker circulation requires that variables be averaged between 30°S and 30°N, latitudes between which net meridional divergence is minimal). A difference plot between the atmosphere-only simulations (Figure 3b) indicates enhanced convection and uplift over the Sunda shelf near 120°E, stronger upper level westerlies over the west central Pacific, increased subsidence over the central eastern Pacific around 150°W, and

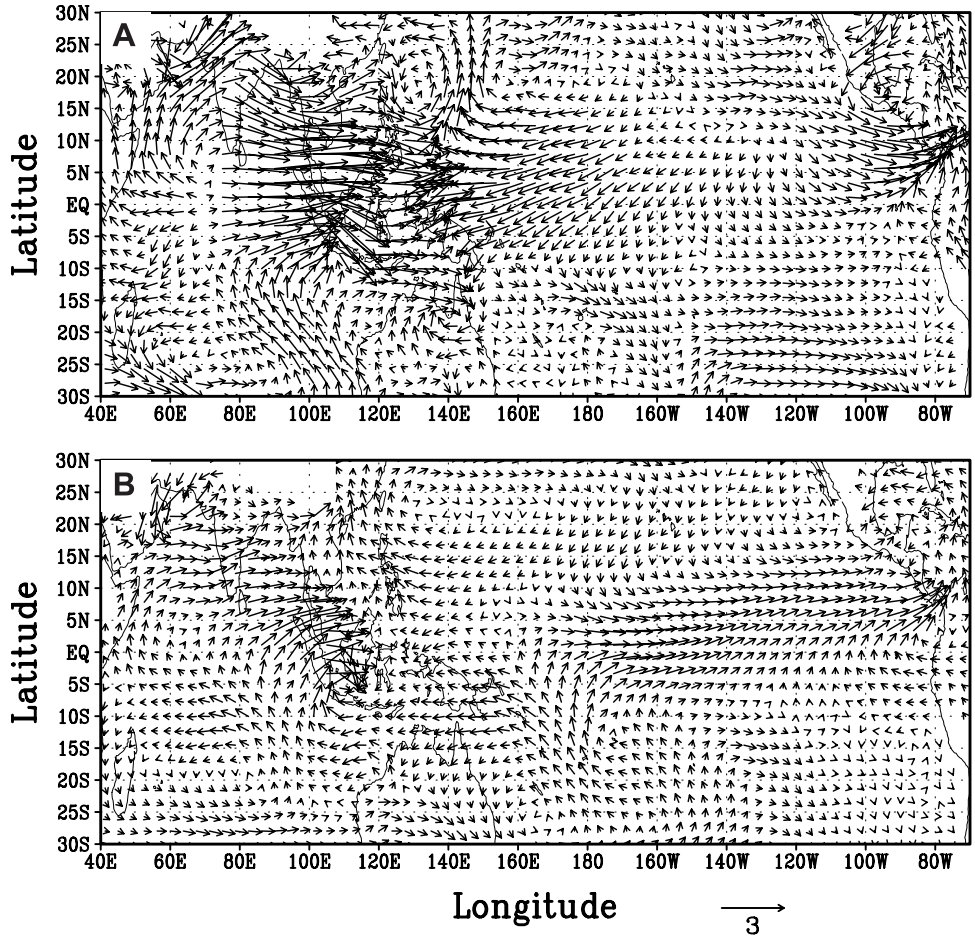

Figure 2. Difference in annual mean 950 mb winds (experiment minus control) for (a) the atmosphere only simulations and (b) the coupled model simulations. Units are m/s, and vectors are scaled as indicated.

anomalous surface westerlies over the far eastern Pacific (130°–80°W). Near the surface these changes are manifested by stronger trade easterlies over the far western Pacific and weaker easterlies over the far eastern Pacific (see Figure 2a). In the coupled model, the same central Pacific subsidence and low-level westerly wind anomalies are simulated (Figure 3c). Persistently dry conditions over the central Pacific during glacial periods have been inferred from accumulated guano deposits [*Quinn*, 1971]. Our results suggest that changes in the mean atmospheric circulation in response to exposure of the Sunda shelf contribute to tropical dryness in this area.

[10] A stream function plot of the 200 mb winds in the control simulation (atmosphere-only) indicates two wave responses over the West Pacific Warm Pool: two Rossby wave anticyclones near 140°–150°E; and a nearly equatorially symmetric westerly Kelvin wave over the central Pacific (Figure 4a). In addition, there is a weaker Rossby wave response to the eastern Pacific cold tongue that gives the flow cyclonic curvature near 120°W. When the Sunda shelf is exposed to radiative heating, anomalous upper level westerlies over the central Pacific are more clearly seen to be an additional Kelvin wave response (Figure 4b), and enhanced upper level convergence over the central Pacific arises from confluence of two anticyclonic circulations (the additional Rossby wave response) near 140°E (Figure 4b). It is this convergence and subsidence that produces the anomalous surface westerlies over the far eastern Pacific (see Figure 3b).

[11] Diagnosis of the coupled model response indicates the same Rossby wave features in the upper troposphere over the Sunda shelf (Figure 4c). The westerly Kelvin wave response is evident over the Indian Ocean but over the central eastern Pacific it is dominated by anomalous easterlies flowing from the far eastern Pacific; their convergence near 160°E contributes to the strong subsidence over the central Pacific (see Figure 3c).

2.2. Tropical Atmosphere-Ocean Interactions

[12] Circulation anomalies over the central eastern Pacific in the coupled model are associated with SST changes, which indicate a ~0.5 degree warming north of the equator under the Intertropical Convergence Zone (ITCZ) (Figure 5). These changes are consistent with an amplification of the anomalous southerly cross-equatorial winds predicted by the atmosphere-only simulations over the far eastern Pacific (Figure 6a). The amplification occurs through coupled atmosphere-ocean dynamics, and consists of a weakening of the trade winds north of the equator (because of Coriolis forces and the fact that the wind anomaly is southerly;

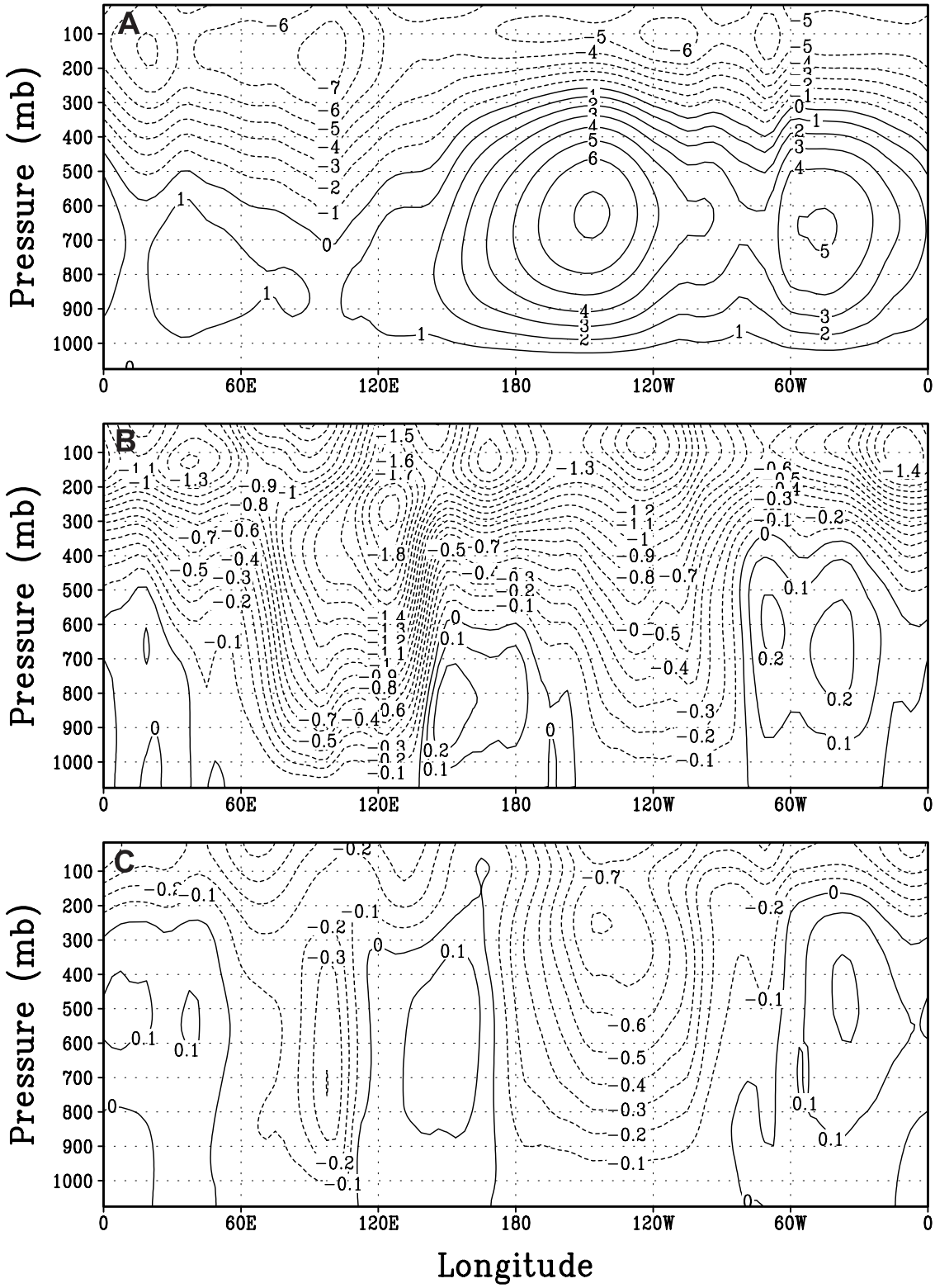

Figure 3. (a) Annual mean Walker circulation in the atmosphere-only control simulation (contour interval is 10^{11} kg/s). The sign is such that a positive value indicates clockwise circulation in the longitude-height plane. (b) The difference between the atmosphere-only simulations (experiment minus control). (c) The difference between the coupled model simulations. The contour interval in Figures 3b and 3c is 0.1×10^{11} kg/s.

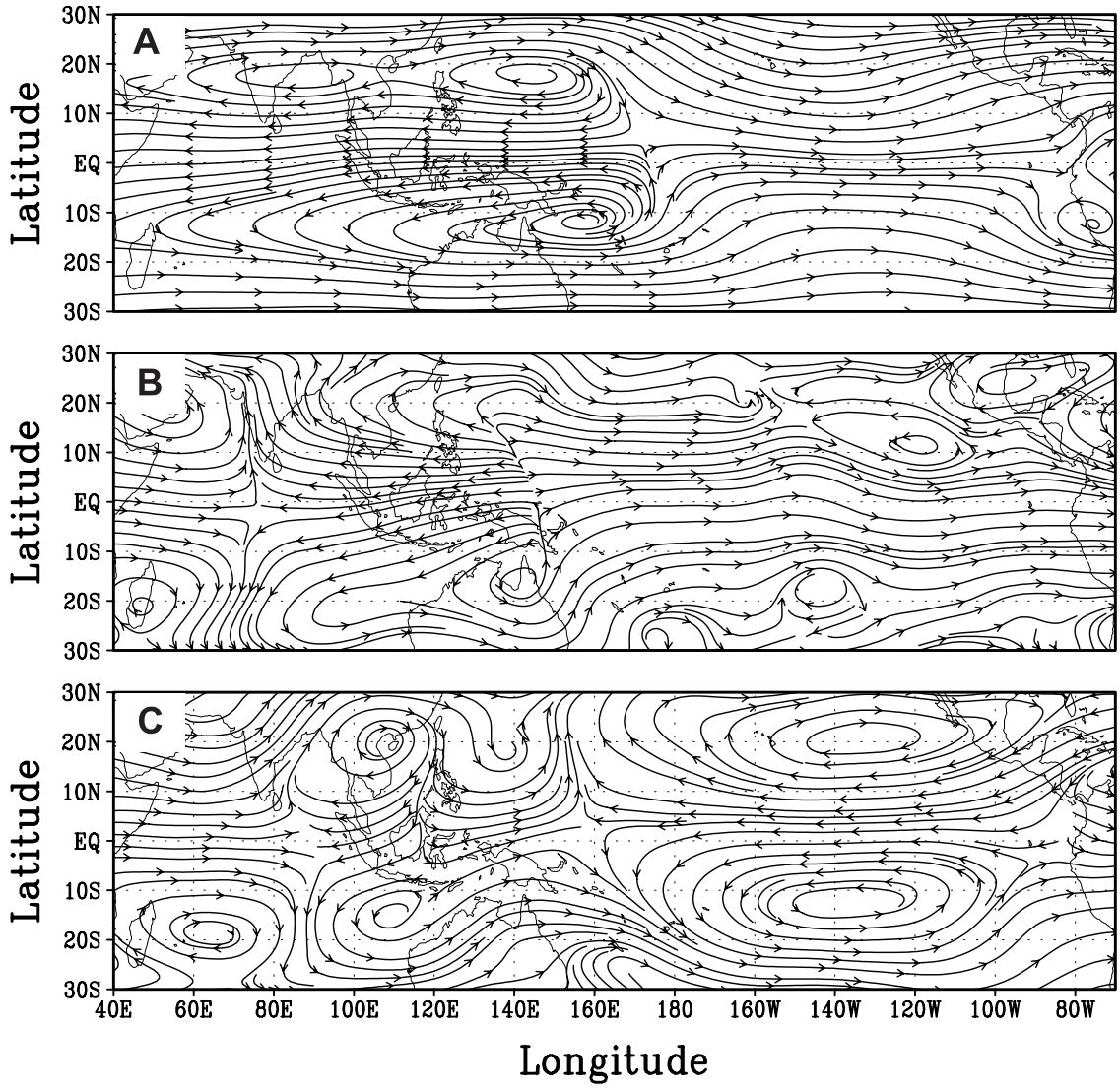

Figure 4. (a) Stream function plot of the annual mean winds at the 200 mb level in the atmosphere-only control simulation. (b) The stream function difference between the atmosphere-only simulations (experiment minus control). (c) The stream function difference between the coupled model simulations.

Figure 6c). Weaker trade winds north of the equator decrease upwelling and evaporation, leading to warmer SST (Figure 6d). This cross-equatorial SST anomaly strengthens the southerly wind anomaly (Figure 6b) and is therefore a positive feedback [*Xie and Philander*, 1994; *Chang and Philander*, 1994]. The atmospheric anomaly (see Figure 6a) and establishment of the consequent coupled atmosphere-ocean anomalies (Figures 6b–6d) are consistent with the westward control dynamics described by *Xie and Saito* [2001] in which atmospheric Rossby waves propagate the anomaly westward and induce a cross-equatorial SST anomaly. In the coupled model simulations, the SST anomaly that develops in the eastern Pacific after two years of model integration propagates westward (Figure 7) at approximately 1 cm/s and is correlated with positive southerly wind anomalies. The initial atmospheric changes over the eastern Pacific are a nonlocal effect of upper level convergence over the central Pacific which is, in turn, caused by the upper troposphere's response to exposure of the Sunda shelf. Coupled dynamics then propagate this signal back to the western Pacific to produce the new climatology.

[13] In the atmosphere-only integration, enhanced convection over the exposed shelf moistens the equatorial troposphere (Figure 8a) through enhanced evaporation of western Warm Pool and Indian Ocean water by strong convergent surface winds. In the coupled model, however, SST cooling south of the equator reduces evaporation to the extent that there is a net drying of the lower tropical atmosphere (Figure 8b). In a global mean, specific humidity changes are on the order of a percent, with a $\sim$1% drying in the coupled model when the shelf is exposed and a $\sim$0.14 degree cooling of the tropical troposphere between 30°S and 30°N. This decrease in global atmospheric water content is not of sufficient magnitude to explain the 10% decrease in the hydrological cycle observed in a simulation of the LGM [*Bush and Philander*, 1998, 1999], but exposure of the shelf is nevertheless one contributing factor to the reduction of

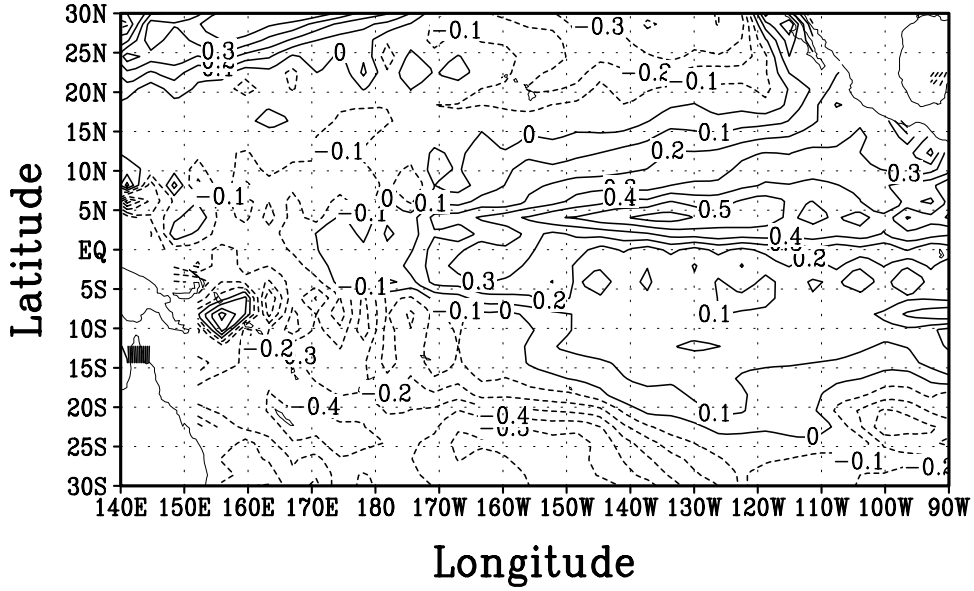

Figure 5. Difference in annual mean SST in the coupled model simulations (experiment minus control). The contour interval is 0.1°C.

tropical water vapor. Other factors that lead to cooling and drying of the tropics are atmospheric CO2, continental ice sheets, and changes in the mean state of the tropical Pacific thermocline.

2.3. Salinity Changes

[14] Exposure of the Sunda shelf therefore increases convection over Indonesia, strengthens the trade easterlies over the far western Pacific, and modifies convection over the Western Warm Pool. In the coupled model simulations, this changes the net freshwater flux and surface salinity of the oceans (Figure 9). When the shelf is exposed, there are decreased salinities over much of the tropical Pacific from the equator to ~15°N (consistent with warmer SST and increased precipitation in the ITCZ) and increased salinities over most of the Pacific south of 5°S (consistent with cooler SST and increased evaporation). Increased salinities at two times of shelf flooding (~15 ka and ~11 ka) have been inferred from at least one South China Sea core [*Pelejero et al.*, 1999]. Although in these simulations there is very little change in salinity in the South China Sea, many other regions surrounding the shelf experience a salinity increase when the shelf is submerged. Large amounts of precipitation over the exposed Sunda shelf produce increased riverine flux of freshwater into the Philippine Sea, the Bay of Bengal, and the Arafura Sea. Flooding of the shelf removes this freshwater source and increases sea surface salinities around the shelf margin.

2.4. Interannual Variability

[15] Changes in the mean state of the tropical Pacific atmosphere-ocean system should impact the period of interannual variability [*Fedorov and Philander*, 2000]. El Niño and La Niña episodes are defined as periods for which the 5-month running mean SST anomalies in the Niño 3.4 region (5°S–5°N; 120°–170°W) are, respectively, 0.4° above or below the climatological mean for a period of at least 6 months. By this definition, the coupled model exhibits an average period of 3.1 years for El Niño episodes when the shelf is submerged and the trade easterlies are strong; when the shelf is exposed and the trades over the eastern Pacific relax, an average period of 4.1 years is simulated. Lengthening of the period between El Niño events when the mean trade wind strength is reduced is generally consistent with results from a sensitivity analysis of the Pacific's neutral stable mode of oscillation [*Fedorov and Philander*, 2000]. A comparison of variances of the Niño 3.4 SST anomaly indices using an F test [*Press et al.*, 1992] indicates a variance increase of 10% when the shelf is submerged and El Niño (ENSO) events are more frequent. A caveat to these results is that ENSO statistics will also be influenced by multidecadal variability that is not so well captured in these simulations.

3. Discussion and Conclusions

[16] Exposure of the Sunda shelf therefore impacts tropical circulation not only over the western Warm Pool but over the entire tropical Pacific. Convective activity is enhanced over Indonesia and reduced over the Warm Pool. The dynamical response to this new site of convection impacts the upper tropospheric circulation both locally and nonlocally. Changes in the mean circulation are in response to anomalous upper tropospheric divergence above the shelf. Near the surface, these changes are characterized by stronger easterly trade winds over the Western Warm Pool and weaker trades over the eastern Pacific. The latter change is a consequence of upper tropospheric convergence and subsidence over the central Pacific.

[17] Increased upwelling and cooler SSTs during glacial times have been suggested for the waters surrounding Nauru (0°32′S, 166°55′E), Ocean (0°52′S, 169°35′E), and the Purdy Islands (2°55′S, 146°25′E) and, in combination with persistently drier conditions, were responsible for the

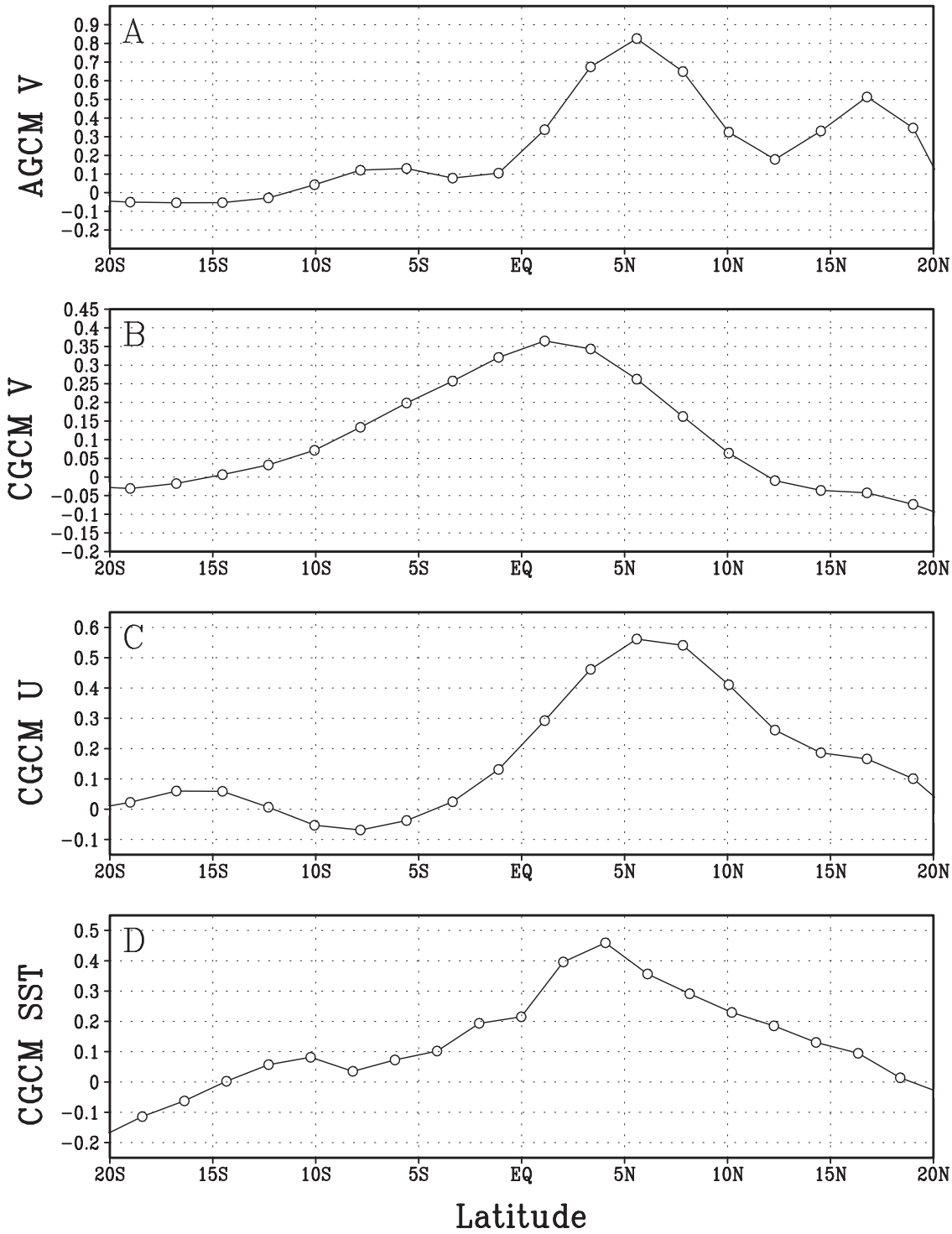

Figure 6. (a) Difference in meridional wind speed over the eastern Pacific (240°–290°E) in the atmosphere-only simulations. (b) Difference in meridional wind speed in the coupled model, averaged over the central east Pacific (220°–290°E). (c) Difference in zonal wind speed in the coupled model, averaged as in Figure 6b. (d) Difference in SST in the coupled model, averaged as in Figure 6b. All differences are experiment minus control. Units are m/s in Figures 6a–6c and °C in Figure 6d.

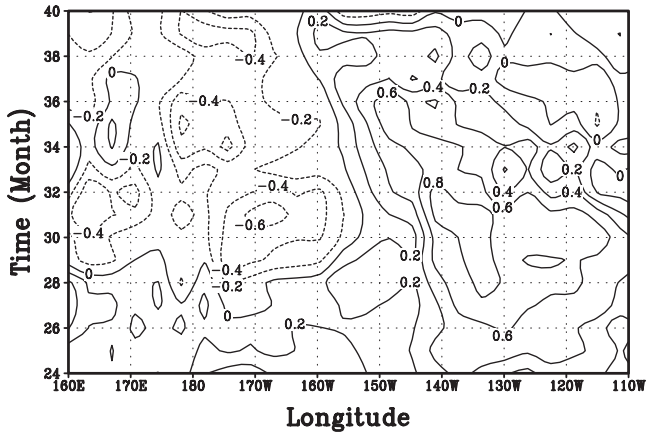

Figure 7. Time versus longitude plot of the difference (experiment minus control) in meridional SST gradient averaged from 5°S to 5°N. The starting time shown corresponds to 2 years after the start of the simulation. Westward propagation of the anomaly is similar to that described by *Xie and Saito* [2001].

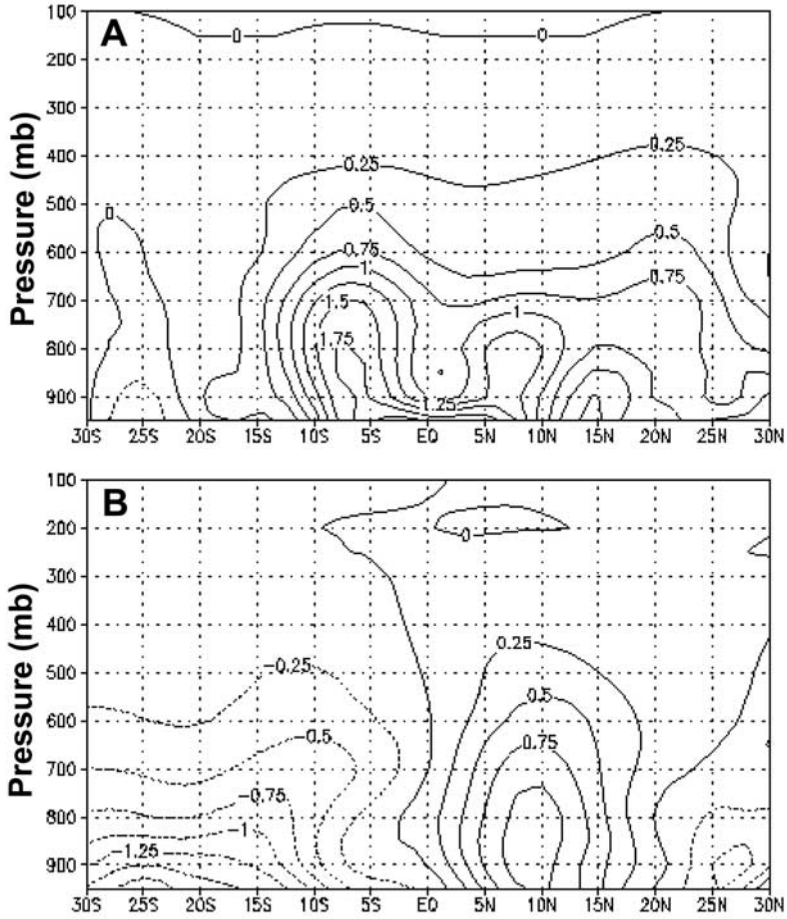

Figure 8. Difference in zonal mean specific humidity between (a) the atmosphere-only simulations and (b) the coupled model simulations. Units are 10^{-4} gm/gm, and contour interval in is 5×10^{-5}.

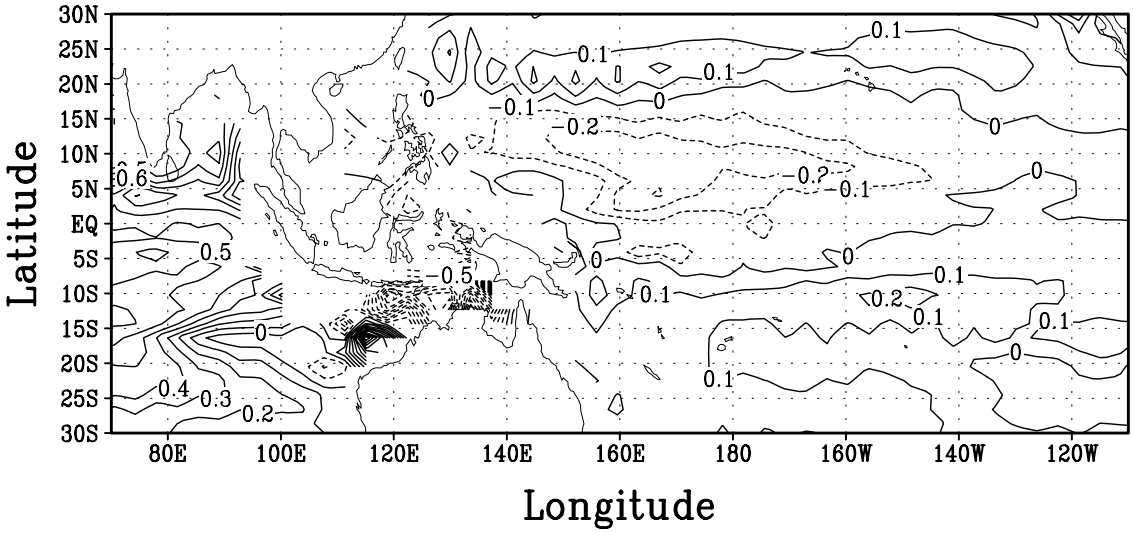

Figure 9. Difference in annual mean SSS in the coupled model simulations (experiment minus control). Units are PSU, and contour interval is 0.2 PSU.

formation of extensive phosphate deposits on these islands [*Quinn*, 1971]. These simulations demonstrate that exposure of the Sunda shelf contributes approximately 10% to the total cooling and drying simulated in the tropical Pacific by *Bush and Philander* [1999]. In comparison to the sensitivity tests by *Broccoli and Manabe* [1987], the impact of Shelf exposure on tropical climate is therefore comparable to the impact of LGM land surface albedo on global climate. Exposure of the large continental shelf in the region of the Gulf of Carpentaria during glacial climates would likely add to these changes.

[18] Results therefore imply that a component of tropical cooling and drying during glacial cycles may be attributed to exposure of the Shelf. Periodic exposure and submergence of the expansive Sunda shelf therefore represents one important mechanism by which the growth and decay of northern hemisphere ice sheets imparts Milankovitch climate cycles to the tropical climate system. In addition, these changes constitute a fundamental shift in the ENSO background state.

[19] **Acknowledgments.** A.B.G.B. acknowledges funding from NSERC G121210769 and the Climate System History and Dynamics Research Network Grant. Funding for R.G.F. from NSF grants OCE94-16971 and OCE98-18349 and from NOAA grant NA06GP0580. The authors would like to thank the anonymous reviewers who took the time to evaluate an earlier version of the manuscript.

References

Broccoli, A. J., and S. Manabe, The influence of continental ice, atmospheric CO_2, and land albedo on the climate of the Last Glacial Maximum, *Clim. Dyn.*, *1*, 87–99, 1987.

Broecker, W., Oxygen isotope constraints on surface ocean temperatures, *Quat. Res.*, *26*, 121–134, 1986.

Bush, A. B. G., and S. G. H. Philander, The role of ocean-atmosphere interactions in tropical cooling during the Last Glacial Maximum, *Science*, *279*, 1341–1344, 1998.

Bush, A. B. G., and S. G. H. Philander, The climate of the Last Glacial Maximum: Results from a coupled atmosphere-ocean general circulation model, *J. Geophys. Res.*, *104*, 24,509–24,525, 1999.

Chang, P., and S. G. H. Philander, A coupled ocean-atmosphere instability of relevance to the seasonal cycle, *J. Atmos. Sci.*, *51*, 3627–3648, 1994.

Colinvaux, P. A., Climate and the Galapagos Islands, *Nature*, *240*, 17–20, 1972.

Fairbanks, R. G., A 17,000 year glacio-eustatic sea level record: Influence of glacial melting rates on the Younger Dryas event and deep-ocean circulation, *Nature*, *342*, 637–642, 1989.

Fairbanks, R. G., The age and origin of the Younger Dryas climate event in Greenland ice cores, *Paleoceanography*, *5*, 937–948, 1990.

Fedorov, A. V., and S. G. H. Philander, Is El Niño changing?, *Science*, *288*, 1997–2002, 2000.

Gill, A. E., Some simple solutions for heat-induced tropical circulation, *Q. J. R. Meteorol. Soc.*, *106*, 447–462, 1980.

Gordon, C. T., and W. Stern, A description of the GFDL global spectral model, *Mon. Weather Rev.*, *110*, 625–644, 1982.

Guilderson, T. P., R. G. Fairbanks, and J. L. Rubenstone, Tropical temperature variations since 20,000 years ago: Modulating interhemispheric climate change, *Science*, *263*, 663–665, 1994.

Hallam, A., *An Outline of Phanerozoic Biogeography*, pp. 178–183, Oxford Univ. Press, New York, 1994.

Hanebuth, T., K. Stattegger, and P. M. Grootes, Rapid flooding of the Sunda shelf: A late-glacial sea-level record, *Science*, *288*, 1033–1035, 2000.

Hostetler, S. W., and A. C. Mix, Reassessment of ice-age cooling of the tropical ocean and atmosphere, *Nature*, *399*, 673–676, 1999.

Keshavamurty, R. N., Response of the atmosphere to sea surface temperature anomalies over the equatorial Pacific and the teleconnections of the Southern Oscillation, *J. Atmos. Sci.*, *39*, 1241–1259, 1982.

Lea, D. W., D. K. Pak, and H. J. Spero, Climate impact of late Quaternary equatorial Pacific sea surface temperature variations, *Science*, *289*, 1719–1724, 2000.

Levitus, S., Climatological atlas of the world ocean, *NOAA Prof. Pap. 13*, 173 pp., U.S. Govt. Print. Off., Washington, D. C., 1982.

Lyle, M. W., F. G. Prahl, and M. A. Sparrow, Upwelling and productivity changes inferred from a temperature record in the central equatorial Pacific, *Nature*, *355*, 812–815, 1992.

Meehl, G. A., P. R. Gent, J. M. Arblaster, B. L. Otto-Bleisner, E. C. Brady, and A. Craig, Factors that affect teh amplitude of El Niño in global coupled climate models, *Clim. Dyn.*, *17*, 515–526, 2001.

Pacanowski, R. C., and S. G. H. Philander, Parameterization of vertical mixing in numerical models of tropical oceans, *J. Phys. Oceanogr.*, *11*, 1443–1451, 1981.

Pelejero, C., M. Kienast, L. Want, and J. O. Grimalt, The flooding of Sundaland during the last deglaciation: Imprints in hemipelagic sediments from the southern South China Sea, *Earth. Planet. Science Lett.*, *171*, 661–671, 1999.

Philander, S. G. H., *El Niño, La Niña, and the Southern Oscillation*, 293 pp., Academic, San Diego, Calif., 1990.

Press, W. H., S. A. Teukolsky, W. T. Vetterling, and B. P. Flannery, *Numerical Recipes: The Art of Scientific Computing*, 963 pp., Cambridge Univ. Press, New York, 1992.

Quinn, W. H., Late Quaternary meteorological and oceanographic developments in the equatorial Pacific, *Nature*, *229*, 330–331, 1971.

Sardeshmukh, P., and B. J. Hoskins, The generation of global rotational flow by steady idealized tropical divergence, *J. Atmos. Sci.*, *45*, 1228–1251, 1988.

Smith, W. H. F., and D. T. Sandwell, Global sea floor topography from satellite altimetry and ship depth soundings, *Science*, *277*, 1956–1962, 1997.

Stute, M., M. Forster, H. Frischkorn, A. Serejo, J. F. Clark, P. Schlosser, W. S. Broecker, and G. Bonani, Cooling of tropical Brazil (5°C) during the Last Glacial Maximum, *Science*, *269*, 379–383, 1995.

Xie, S.-P., and S. G. H. Philander, A coupled ocean-atmosphere model of relevance to the ITCZ in the eastern Pacific, *Tellus, Ser. A*, *46*, 340–350, 1994.

Xie, S.-P., and K. Saito, Formation and variability of a northerly ITCZ in a hybrid coupled AGCM: Continental forcing and oceanic-atmospheric feedback, *J. Clim.*, *14*, 1262–1276, 2001.

A. B. G. Bush, Department of Earth and Atmospheric Sciences, 126 Earth Sciences Building, University of Alberta, Edmonton, Alberta, Canada T6G 2E3. (andrew.bush@ualberta.ca)

R. G. Fairbanks, Department of Earth and Environmental Sciences of Columbia University and Lamont Doherty Earth Observatory, P. O. Box 1000, 61 Route 9W, Palisades, NY 10964-1000, USA.